Evolution of Glutamate Dehydrogenase Regulation of Insulin Homeostasis Is an Example of Molecular Exaptation†

Aron Allen,‡,§ Jae Kwagh,||,§ Jie Fang,|| Charles A. Stanley,|| and Thomas J. Smith*,‡

The Donald Danforth Plant Science Center, 975 North Warson Road, St. Louis, Missouri 63132, and The Children's Hospital of Philadelphia, Endocrinology Division, Room 802, 3516 Civic Center Boulevard, Philadelphia, Pennsylvania 19104

Received June 8, 2004; Revised Manuscript Received August 13, 2004

ABSTRACT: Glutamate dehydrogenase (GDH) is found in all organisms and catalyzes the oxidative deamination of glutamate to 2-oxoglutarate. While this enzyme does not exhibit allosteric regulation in plants, bacteria, or fungi, its activity is tightly controlled by a number of compounds in mammals. We have previously shown that this regulation plays an important role in insulin homeostasis in humans and evolved concomitantly with a 48-residue "antenna" structure. As shown here, the antenna and some of the allosteric regulation first appears in the Ciliates. This primitive regulation is mediated by fatty acids and likely reflects the gradual movement of fatty acid oxidation from the peroxisomes to the mitochondria as the Ciliates evolved away from plants, fungi, and other protists. Mutagenesis studies where the antenna is deleted support this contention by demonstrating that the antenna is essential for fatty acid regulation. When the antenna from the Ciliates is spliced onto human GDH, it was found to fully communicate all aspects of mammalian regulation. Therefore, we propose that glutamate dehydrogenase regulation of insulin secretion is a example of exaptation at the molecular level where the antenna and associated fatty acid regulation was created to accommodate the changes in organelle function in the Ciliates and then later used to link amino acid catabolism and/or regulation of intracellular glutamate/glutamine levels in the pancreatic β cells with insulin homeostasis in mammals.

Glutamate dehydrogenase (GDH)[1] is found in all organisms and catalyzes the reversible oxidative deamination of L-glutamate to 2-oxoglutarate using NAD(H) and/or NADP(H) as a coenzyme (*1*). However, only mammalian GDH has been shown to exhibit complex allosteric regulation. The structures of several bacterial (*2*−*5*) and mammalian (*6*−*9*) forms of the enzyme have been determined to date. Despite modest homology, they share a number of important structural features. All of these enzymes are homohexameric, exhibiting 32 symmetry, and the first ~200 residues form the core, "glutamate-binding" domain. On top of this domain is a "NAD-binding" domain that rotates ~20° during catalysis (*7*). Unique to the animal structures, there is a 48-residue "antenna" that protrudes above this NAD-binding domain (Figure 1). The three antennae within the trimers intertwine and move with respect to each other as the NAD-binding domain opens and closes (*7*).

In mammalian GDH, the rate-limiting step changes depending upon the enzymatic conditions. At neutral pH and low coenzyme and substrate concentrations, the rate-limiting step is hydride-transfer and/or the conformational changes associated with this process (e.g., the movement of the NAD-binding domain). In the oxidative deamination reaction at high pH and high substrate concentrations, glutamate binds to the enzyme before the NAD(P)H molecule dissociates from the catalytic cleft, thereby forming a tightly bound NAD(P)H·GLU abortive complex. Under these conditions, hydride transfer is no longer rate-limiting but rather the release and reconciliation of the abortive complex. In the reductive amination reaction, the analogous $NAD(P)^+$·αKG abortive complex is formed at high substrate concentrations and low pH (*10*).

The two major opposing allosteric regulators, ADP and GTP, appear to exert their effects via these abortive complexes. ADP is an activator believed to act, at least in part, by destabilizing the abortive complex (*11*, *12*). In contrast, GTP is a potent inhibitor and is thought to act by stabilizing abortive complexes (*13*). GTP binding is antagonized by phosphate (*14*) and ADP (*15*) but is proposed to be synergistic with NADH bound in a noncatalytic site (*14*). Finally, ADP and GTP bind in an antagonistic manner (*15*) either because of steric competition or because of competing effects on abortive complex formation. In our previous structural studies, we proposed that these regulators cause

† This work was supported by Grants from the National Institutes of Health (GM10704 and DK53012) to T.J.S. and C.A.S., respectively.

* To whom correspondence should be addressed. E-mail: tsmith@danforthcenter.org. Phone: (314) 587-1451. Fax: (314) 587-1551.

‡ The Donald Danforth Plant Science Center.

§ To be considered co-first authors.

|| The Children's Hospital of Philadelphia.

[1] Abbreviations: GDH, glutamate dehydrogenase; tGDH, *Tetrahymena thermophila* glutamate dehydrogenase; hGDH, human glutamate dehydrogenase; pGDH, *Paramecium tetraurelia* glutamate dehydrogenase; HI/HA, hyperinsulinism/hyperammonemia; EDTA, ethylenediaminetetraacetic acid; EGTA, ethylene glycol-bis(*b*-aminoethyl ether)-*N*,*N*,*N*′,*N*′-tetraacetic acid; GTP, guanosine triphosphate; ADP, adenosine diphosphate; cGDH, *Clostridium symbiosum* glutamate dehydrogenase; NAD, β-nicotinamide adenine dinucleotide; NADP, β-nicotinamide adenine dinucleotide 2′-phosphate; TNP-ADP, 2′-(or-3′)-*O*-(trinitrophenyl) adenosine 5′-diphosphate.

10.1021/bi048817i CCC: $27.50
Published on Web 10/23/2004

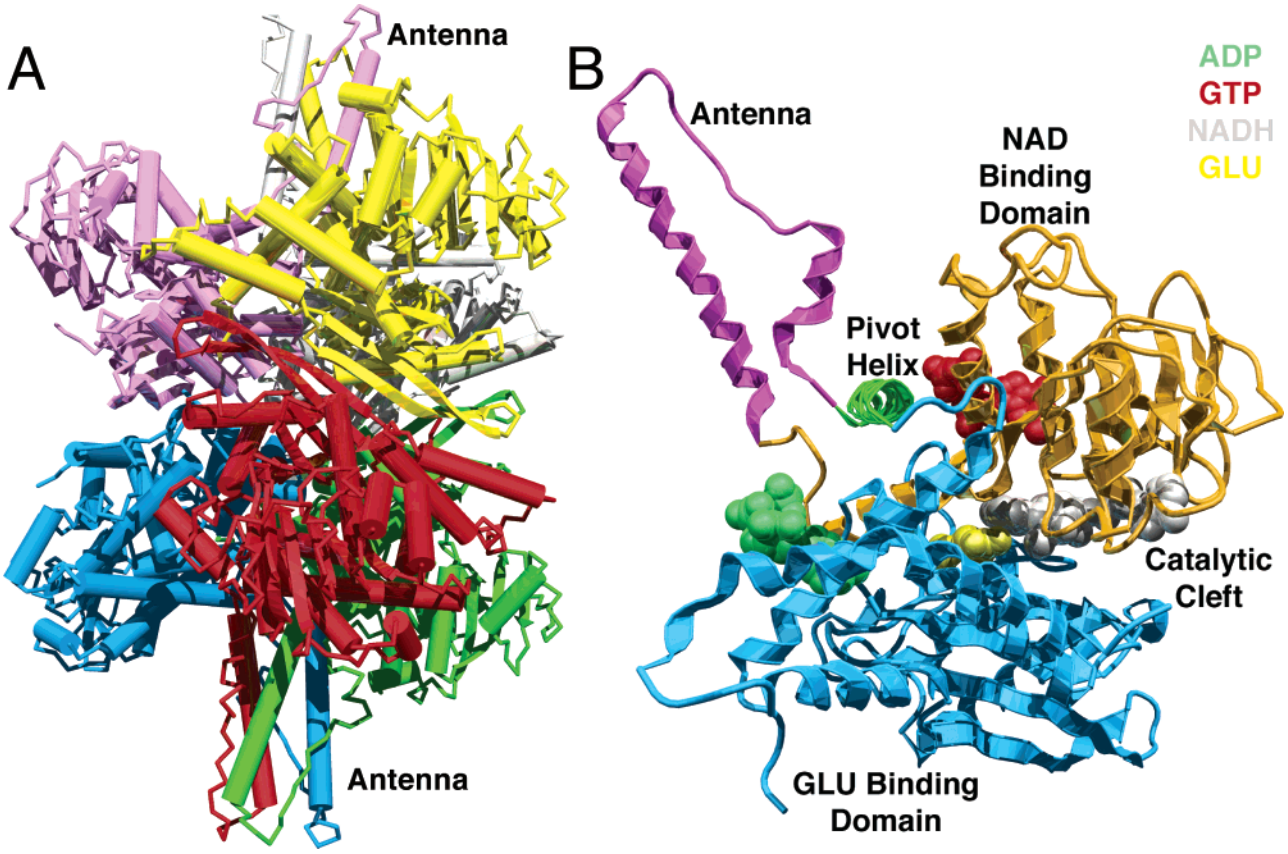

FIGURE 1: Structure of mammalian GDH. (A) Shown here is a ribbon diagram of the entire hexamer with the subunits represented by different colors. (B) One of the six subunits of bGDH with the 3-fold axis approximately vertical on the page toward the left-hand side of the figure. The 2-fold axes are perpendicular to the 3-fold and at the bottom of the figure. The glutamate-binding domain, NAD-binding domain, antenna, and pivot helix are colored blue, orange, mauve, and green, respectively. The space-filling structures of bound GTP, ADP, NADH, and glutamate are colored red, green, silver, and yellow, respectively.

these effects by modulating the dynamics of the movement of the NAD-binding domain (*7*, *8*).

A major complication to analysis of GDH has been that bovine GDH has a second coenzyme site on each subunit. This site binds NAD(H) ~10-fold better than NADP(H) (*16*, *17*), with the reduced form binding better than the oxidized form (*18*). Reduced coenzyme binding inhibits the reaction (*16*, *17*), while oxidized coenzyme binding has been suggested to cause activation (*19*). These results are hard to reconcile because our structural work has shown that both NAD and NADH bind to the same site (*9*). Another point of contention is that NADH binds to the second coenzyme site with an affinity of ~60 μM (*17*), yet NADH inhibition of the steady-state reaction is only observed at very high concentrations (~1 mM) of NADH (*17*, *20*, *21*). Therefore, it is not clear whether NADH inhibition is due to NADH binding to the second coenzyme site and whether such inhibition is physiologically relevant.

Leucine, as well as some other monocarboxylic acids, have been shown to activate mammalian GDH (*22*) by increasing the rate-limiting step of coenzyme release in a manner similar to ADP (*23*). However, because ADP and leucine activation were shown to be synergistic, these activators apparently do not bind to the same site (*23*). Because leucine is a weak substrate for GDH, clearly one binding site is the active site. The major question is whether there is a second, allosteric, leucine-binding site. Palmitoyl-CoA (*24*) and diethylstilbestrol (*25*) are inhibitors of mammalian GDH, but nothing is known about their binding location.

Our recent studies on the hyperinsulinism and hyperammonemia (HI/HA) syndrome in humans have suggested one possible role for complex mammalian allosteric regulation. HI/HA is caused by mutations in GDH that cause the loss of GTP inhibition (*26*, *27*). It was further suggested that, in the β cells of the pancreas, the increased glutamate to 2-oxoglutarate conversion will increase the respiration rate via the Krebs cycle, thereby increasing the ATP/ADP ratio. This, in turn, leads to inhibition of K^+-channel activity and results in excessive release of insulin. Studies using isolated islets from normal animals show that leucine, unlike all other amino acids, only provokes insulin secretion when added to islets that have been deprived of glucose for more than 120 min. This suggests that leucine stimulation requires a "run-down" of β-cell energy levels. That is, incubation in the absence of glucose presumably lowers the phosphate potential and, according to our current model for GDH regulation, releases both GTP- and ATP-mediated inhibition. This concept is further supported by reports that leucine also stimulates glutamate oxidation by isolated islets (*28*). These observations implicate GDH as the key sensor for protein-mediated insulin secretion, analogous to the role of glucokinase as the sensor for glucose-regulated insulin secretion (*29*).

The purpose of the work described here is to use an evolutionary approach to better understand the structure/function relationships of mammalian glutamate dehydrogenase by studying how its allosteric features have developed over the epochs. As is shown here, GDH from the Ciliates is an evolutionary intermediate between animals and the other

kingdoms. From the recently released results of the *Tetrahymena* Genome Project (www.lifesci.ucsb.edu/~genome/Tetrahymena), we observe that *Tetrahymena thermophila* GDH (tGDH) is predicted to have an antenna-like protrusion similar to that found in animal GDH. Like mammalian GDH, tGDH exhibits ADP activation and inhibition by palmatoyl CoA. However, like bacterial GDH, tGDH is coenzyme-specific [NAD(H)] and is not regulated by GTP or leucine. Mutagenesis studies on human GDH clearly demonstrate that the antenna structure is required for GTP, ADP, and palmitoyl-CoA regulation. When the Ciliate antenna is spliced onto mammalian GDH, the hybrid form of the enzyme has a fully functional repertoire of mammalian allostery. Therefore, Ciliate GDH was capable of being regulated by GTP, but apparently, there was no selective pressure to create the GTP-binding site. Because GTP and leucine have been shown to be crucial for GDH-mediated regulation of insulin secretion, we propose that allostery in GDH was created in two major steps that were due to different evolutionary pressures. The Ciliates first created the antenna to link fatty oxidation to amino acid catabolism because β-oxidation of fatty acids moved from the peroxisomes to the mitochondria. The second step of evolution was to add leucine and GTP regulation because animals needed to use GDH to link insulin homeostasis with amino acid catabolism and/or to regulate intracellular concentrations of glutamine/glutamate within the β cells of the pancreas.

MATERIALS AND METHODS

tGDH Production. T. thermophila was cultured in SSP media (2% peptone, 0.1% yeast extract, 0.2% glucose, and 0.003% sequestrene) containing 50 μg/mL ampicillin at room temperature for 2−3 days. The cells were harvested by centrifugation at 4K rpm in a Beckman JLA-9.100 rotor for 20 min. The cell pellets were resuspended in lysis buffer containing 0.1 M sodium phosphate at pH 7.0, 0.1 M KCl, 2 mM EDTA, 1 mM phenyl methylsulfonylfloride, and 5 mM EGTA. The cells were lysed by sonication, and the cellular debris was removed by centrifugation. The supernatant was pooled, and the DNA was precipitated by the addition of protamine sulfate to a final concentration of 0.2%. After the precipitate was removed by centrifugation, the supernatant was pooled and the enzyme precipitated at 4 °C overnight with a 60% (final concentration) of ammonium sulfate. The tGDH activity was found to be stable for long periods of time under these conditions. The protein precipitate was then collected by centrifugation, and the pellet was resuspended in 0.1 M sodium phosphate buffer at pH 7.0 that contained freshly prepared protease inhibitor cocktail (Sigma Corporation) and dialyzed against the same.

The enzyme was rapidly purified using three chromatography steps. The majority of the initial contaminants were removed using a Pharmacia HiTrap Blue HP column. The dialyzed sample was loaded and washed in the same 0.1 M sodium phosphate buffer at pH 7.0 that contained the protease cocktail. GDH was eluted from the column using a gradient of NaCl that went from 0 to 2 M in 30 mL. GDH activity of the various fractions were measured via the oxidative deamination reaction using 1 mM NAD and 40 mM glutamate in 0.1 M sodium phosphate buffer at pH 7.0. The fractions containing GDH activity were pooled and dialyzed overnight against 20 mM sodium phosphate buffer at pH 7.0. Mono-Q anion-exchange chromatography was then performed using a NaCl gradient that went from 0 to 1 M in 20 min at a flow rate of 1 mL/min. Fractions exhibiting GDH activity were pooled and examined using SDS−PAGE analysis. The final step in purification was size-exclusion chromatography using a 300 mL, S-300 Sephadex size-exclusion column and 0.1 M sodium phosphate buffer at pH 7.0 and at a flow rate of 1.5 mL/min. The active fractions were found to be pure according to both SDS−PAGE and MALDI analysis. Immediately after purification, the tGDH was stored as a 60% $(NH_4)_2SO_4$ suspension.

Kinetic Analyses. The bovine GDH (bGDH) used in these studies was obtained as an aqueous $(NH_4)_2SO_4$ suspension from Sigma−Aldrich Chemical Co. Prior to kinetic analysis, aliquots of both tGDH and bGDH were extensively dialyzed against 0.1 M sodium phosphate buffer at pH 7.0 that contained 1 mM EDTA. The enzyme concentrations were adjusted to 1 mg/mL, and the amount of enzyme added to the reaction mixture was adjusted to yield optimal steady-state velocity measurements. Coenzyme and ADP solutions were made immediately prior to use. Enzyme assays were performed by monitoring reduced coenzyme absorbance at 340 nm using a Shamadzu UV-1601 spectrophotometer. All reactions were performed in 3 mL volumes in 0.1 M sodium phosphate buffer at the pH noted in the figure captions. The oxidative deamination reactions were performed at pH 8.0 in the presence of 50 mM glutamate and 0.2 mM NAD. The reductive amination reactions were performed at pH 7.0 in the presence of 0.1 mM NADH, 50 mM NH_4Cl, and 5 mM 2-oxoglutarate. Data were analyzed using GraphPad Prism (www.graphpad.com).

2′-(or-3′)-O-(Trinitrophenyl) Adenosine 5′-Diphosphate (TNP-ADP) Binding Analyses. Previous studies have shown that TNP-ADP binds to and activates mammalian GDH with an efficacy comparable to authentic ADP (*30*). Therefore, TNP-ADP was employed here to measure ADP-binding affinity to wild-type bGDH and the R463A hGDH mutant. Purified R463A hGDH and bGDH samples were dialyzed extensively against 0.1 M sodium phosphate buffer at pH 7.0 that contained 1 mM EDTA, and the protein concentrations were adjusted to 0.33 mg/mL assuming an extinction coefficient of 0.93 mL cm^{-1} mg^{-1}. Titration of binding sites was measured fluorometrically by successive additions of TNP-ADP to the same cuvette, and the fluorescence intensity was recorded after each addition. Fluorescence intensity was measured using a Cary Eclipse fluorometer with the excitation and emission wavelengths set at 408 and 540 nm, respectively. The slit widths for both settings were 10 nm, and each fluorescence reading was averaged over 5 s. The data were analyzed using Graphpad Prism to correct for the slight nonlinearity at higher TNP-ADP concentrations caused by inner-filter effects, and then the ΔF profiles were fitted to the binding equilibrium equation ($\Delta F = [\text{TNP-ADP}]B_{max}/(K_d + [\text{TNP-ADP}])$) using nonlinear regression analysis.

Cloning an "Antenna-less" Form of hGDH. The hGDH antenna was replaced with the corresponding region from *Clostridium symbiosum* GDH (cGDH) using the overhanging, overlapping PCR technique, and the primers are shown in Table 1. The nucleotides underlined in this table represent the loop that cGDH has instead of the antenna. In the PCR 1 reaction, the GDH wild-type mature nucleotide sequence in the pET21a(+) vector was used as a template. The

Table 1: PCR Primer Sequences for the Hybrid Construct

PCR 1	sense vector upstream primer	5′-atgccggccacgatgcgtccggcgtaga-3′
	antisense overhanging primer	5′-cttcctctgctgtaccgctgacatgatttagattcttcag-3′
PCR 2	sense overhanging primer	5′-gctggacagcagaggaagagaaagacatcgtgcactctggcttg-3′
	antisense T7 terminator primer	5′-gctagttattgctcagcgg-3′
PCR 3	sense vector upstream primer of PCR 1	5′-atgccggccacgatgcgtccggcgtaga-3′
	antisense T7 terminator primer of PCR 2	5′-gctagttattgctcagcgg-3′

Table 2: PCR Primer Sequences for the *Ciliate* Hybrid Construct

sense pGDH antenna primer	5′-ggc tat tca aat ttc tac tgg ttt gag agt aga tgt tac caa aaa cca aca agc tgc caa act tct tga agg tcc ttc aGG AGA AAG ACA TCG TGC-3′
antisense pGDH antenna primer	5′- act ctc aaa cca gta gaa att tga ata gcc tct agc aat ttg tatttg gaa gtt tct tcc cat ctt ctg gtcatt ctt ccA TTT AGA TTC AAC CAC T-3′

pET21a(+) upstream primer and antisense overhanging primer were used to amplify GDH from upstream of the N terminus of GDH to the start of the antenna (residue 398). During this process, the 5′ section of antisense primer coding for the cGDH connection peptide (underlined) overhung and the remaining primer bases annealed to the GDH template. In the PCR 2 reaction, a sense overhanging primer and pET T7 terminator primer were applied to the segment of GDH downstream of the antenna region (residue 449) and continued until the vector T7 terminator region. In the PCR 3 reaction, equal amounts of the products from the first two reactions were added together and 7 cycles of a fill-in PCR reaction was used. This fragment was then amplified using the sense primer from the PCR 1 reaction and the antisense primer from the PCR 2 reaction. Using the *Nde*I site at the 5′ region and *Not*I site at the 3′ region in this fragment, this modified form of hGDH was ligated into the pET21a(+) vector. The resulting "antenna-less" form of GDH was then expressed and purified as previously described (*31*).

Cloning the Ciliate/hGDH Hybrid. For this construct, the antenna-less plasmid was used as a PCR template. In the first PCR reaction, the sense paramecium GDH (pGDH) antenna primer (Table 2) was used with antisense T7 terminator primer (Table 1) to combine the C-terminal portion of the pGDH antenna with the C-terminal portion of hGDH. The N-terminal portion of hGDH and the pGDH antenna were combined using the sense vector upstream primer (Table 1) and the antisense pGDH antenna primer. These two fragments were combined with a fill-in PCR reaction and amplified using the sense vector upstream primer and the antisense T7 terminator primer. As above, this modified form of hGDH was ligated into the pET21a-(+) vector, and this hybrid form of GDH was expressed and purified as previously described (*31*).

RESULTS

Comparison of Ciliate and Mammalian GDH Sequences. Using the results from the *Tetrahymena* Genome Project, annotated fragments of tGDH were aligned to human GDH. As shown in Figure 2, tGDH is 41% identical and 58% similar to hGDH and 61% identical and 75% similar to paramecium GDH. It should be noted that the N-terminal portion of pGDH is missing from the database sequence. In the case of tGDH, the sequence shown has a calculated molecular weight of 53 767 Da, and the major peak from MALDI analysis had a molecular weight of 53 660 Da (data not shown). Therefore, the sequence shown here is likely to be that of the mature protein after mitochondrial import and processing. As was previously noted in the case of pGDH (*8*), the major feature in tGDH that makes it more like hGDH than bacterial GDH is the antenna domain.

There are, however, several regions of key differences between the amino acid sequences of GDH from Ciliates and animals as denoted by arrows in Figure 2. From the sequence alignment, it seemed unlikely that Ciliate GDH can bind GTP. The majority of the interactions between mammalian GDH and GTP are between basic residues and the γ-phosphate of GTP (*9*). In Figure 2, three of the more crucial residues are denoted by arrows 1−3. These three basic residues in hGDH are either acidic or hydrophobic residues in Ciliate GDH, and therefore, it seemed unlikely that GTP could bind to and inhibit Ciliate GDH. In particular, it should be noted that H454 (arrow 3) is one of the sites of point mutations that leads to the loss of GTP inhibition in HI/HA patients (*32*).

From the sequence alignments, it was less clear whether Ciliate GDH could bind ADP. In contrast to GTP, the majority of the ADP interactions with mammalian GDH are via the purine ring (*8*, *9*). Our previous studies had shown that R463 on the pivot helix rotated down onto the bound ADP as the catalytic mouth opens (*8*). This interaction is important in mammalian GDH because we have shown that the R463A mutation blocks ADP activation (*31*). However, R463 is replaced by a valine in both pGDH and tGDH (arrow 4). From this alone, it would follow that Ciliate GDH would not be affected by ADP; however, this was not the case as detailed below. Finally, the outermost tip of the antenna in Ciliate GDH is seven residues shorter than that found in mammalian GDH (arrow 5). This could be of significance because chemical modification of this region in bGDH affects allostery (*33*).

Examination of Negative Cooperativity and Substrate Inhibition in the Oxidative Deamination Reaction. Mammalian glutamate dehydrogenase exhibits significant deviations from Michaelis−Menton kinetics. When NAD or NADP is varied in the oxidative deamination reaction, there are significant breaks in the Lineweaver−Burke plots that have been ascribed to negative cooperative binding of the coenzyme to the enzyme (*34*−*37*). As shown in Figure 3 and summarized in Table 3, tGDH exhibits similar behavior with a break from linearity occurring at ~0.2 μM NAD. However, the change in K_m for NAD is not nearly as pronounced in tGDH as it is in bGDH; an approximate 2-fold versus 6-fold change in K_m. While these differences might be ascribed to nonidentical antenna domains, it should be noted that an 8-fold change in the K_m for NAD was

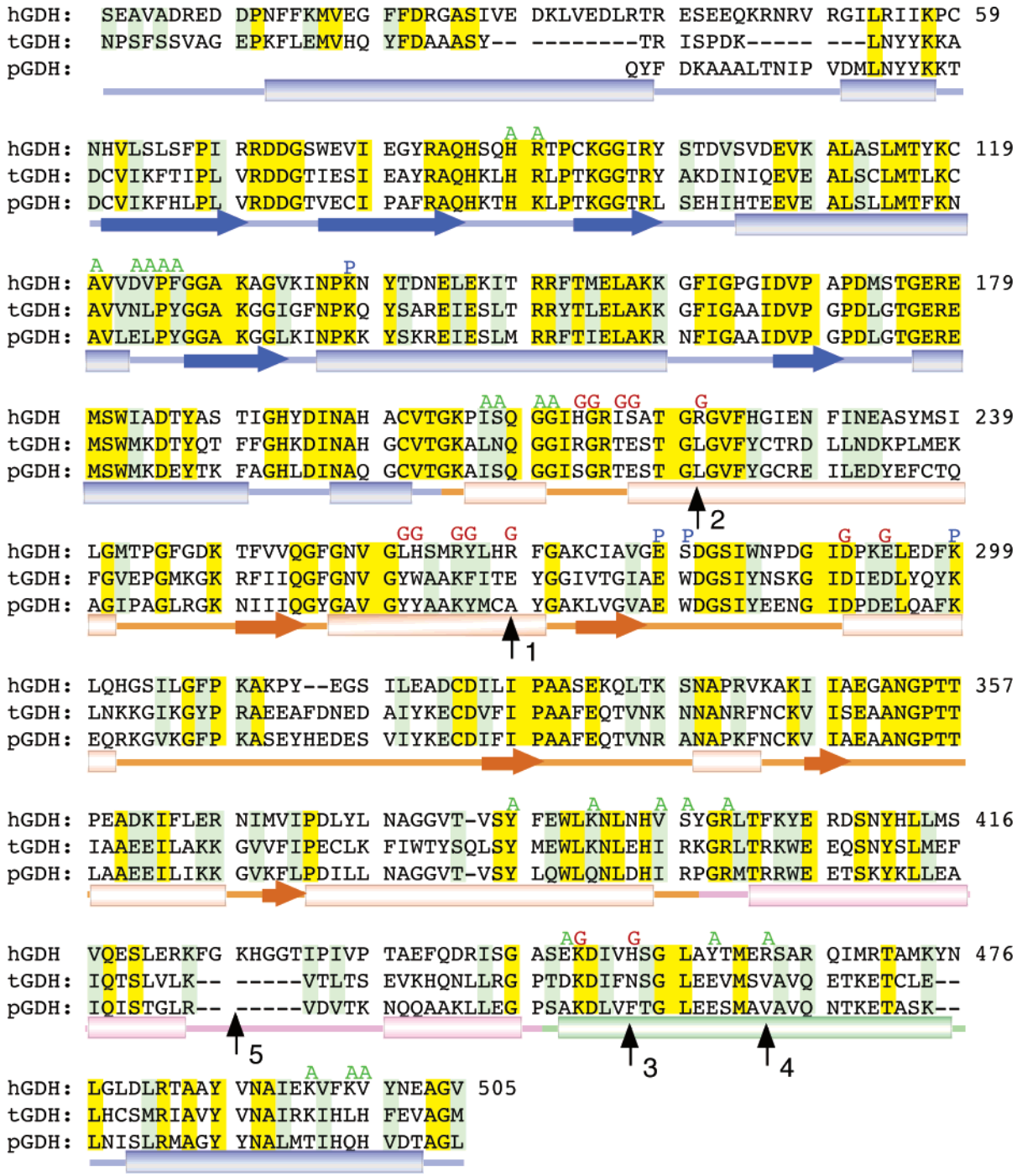

FIGURE 2: Sequence alignment of hGDH (Genbank accession number BC040132), tGDH, and pGDH (Genbank accession number AAG15493). In this figure, the sequences were aligned using BLAST. Immediately below the alignments are lines, cylinders, and arrows representing random coils, helices, and β sheets, respectively, based on the structure of apo hGDH. The coloring of these secondary structures is the same domain-based coloring scheme as used in Figure 1. The residues that are identical among the three forms of GDH are highlighted in yellow, and those that are similar are highlighted in pale green. The green "A"s, red "G"s, and blue "P"s, immediately above some of the aligned residues, denote residues involved in ADP, GTP, and the ribose-phosphate of NADPH, respectively. Arrows labeled 1−3 are the residues that are likely to be responsible for the lack of GTP binding in tGDH. In bGDH, these residues are involved in γ-phosphate interactions. The arrow labeled "3" is the location of one of the HI/HA mutations (H454Y) that is responsible for the abrogation of GTP inhibition. The arrow labeled "4" is the location of our previous site-directed mutation (R463A) that abrogated ADP activation. Finally, the arrow labeled "5" shows that the tip of the protista antenna region is significantly shorter than that of mammalian GDH.

previously reported for cGDH, a form of GDH that does not have an antenna (*38*). Another notable deviation from Michaelis−Menton kinetics with mammalian GDH is substrate inhibition by glutamate at pH 8.0 (*10*). As shown in Figure 3 and summarized in Table 4, tGDH is very similar to mammalian GDH in this regard as well. A slight deviation from linearity was also observed at high glutamate concentrations with cGDH at high pH (*38*). Therefore, it is possible that these two anomalies in steady-state kinetics may not be a manifestation of the antenna domain.

Effects of Allosteric Regulators on tGDH Activity. Steady-state analyses of the effects of allosteric regulators demonstrate that tGDH is an intermediate between bacterial and mammalian forms of the enzyme (Figure 4 and Table 5).

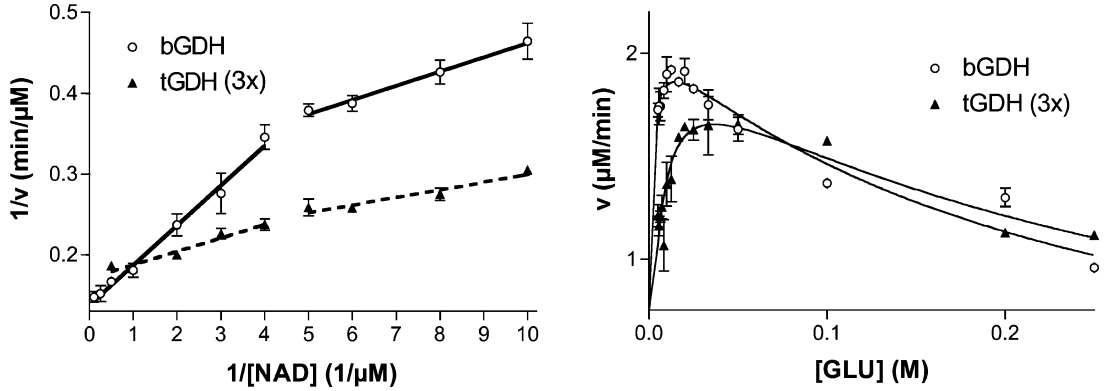

FIGURE 3: Examination of negative cooperativity and substrate inhibition in the oxidative deamination reaction. On the left is a Lineweaver−Burke plot of the oxidative deamination reaction at varied NAD concentrations. As has been previously observed (*34*, *37*), there is a marked break in this plot at ~0.2 μM and a hallmark of negatively cooperative binding of NAD. Therefore, the data were divided into two regions for K_m and V_{max} calculations and are summarized in Table 3. On the right is a plot of the velocity of the steady-state velocity at various glutamate concentrations. As has been previously observed for mammalian GDH (*10*), there is apparent substrate inhibition at high glutamate concentrations. Here, the data were fitted to a two-site binding equation as summarized in Table 4. In both graphs, the tGDH velocities have been multiplied by 3 for presentation purposes.

Table 3: Summary of Kinetic Analysis of the Oxidative Deamination Reaction at Varied NAD Concentrations as Shown in Figure 3[a]

enzyme	[NAD] range	K_m (μM)	V_{max} (μM/min)
bGDH	high [NAD]	0.357 (0.041)	7.22 (0.31)
	low [NAD]	0.061 (0.018)	3.49 (0.27)
tGDH	high [NAD]	0.097 (0.013)	1.94 (0.05)
	low [NAD]	0.046 (0.005)	1.62 (0.10)

[a] Linear regression analysis results of two regions of the NAD-varied Lineweaver−Burke plots. The numbers in parentheses show the standard error in the various calculated values.

Table 4: Summary of Kinetic Analysis of the Oxidative Deamination Reaction at Varied Glutamate Concentrations as Shown in Figure 3[a]

enzyme	V_{max} (μM/min)	K_a (mM)	K_i (mM)
bGDH	2.09 (0.06)	0.92 (0.26)	238 (28)
tGDH	0.69 (0.04)	0.46 (0.75)	291 (55)

[a] These data were analyzed using nonlinear regression analysis using the following equation: $V = (V_{max}[GLU])/(K_a + [GLU](1 + [GLU]/K_i))$, where V_{max} is the maximum velocity of the reaction, K_a is the apparent disassociation constant for glutamate, and K_i is the apparent disassociation constant for glutamate during the substrate inhibition phase of the reaction. The numbers in parentheses represent the standard error in the various values.

Like mammalian GDH, tGDH is inhibited by palmitoyl-CoA (Figure 4D) and activated by ADP (Figure 4A). In the case of ADP, the apparent binding constant and maximal activation are nearly identical to that of bGDH. Therefore, despite the fact that the residue equivalent to the essential R463 is a valine in the Ciliates, ADP is as effective in activating tGDH as bGDH. In contrast, palmitoyl-CoA inhibits bGDH to more than 98%, while it only inhibits tGDH by ~60%. With palmitoyl-CoA, there is a slight activation of the wild-type enzyme in this oxidative deamination reaction at very low concentrations. This was not observed in the case of tGDH, nor was it as pronounced in the reductive amination reaction for wild-type GDH (Figure 5D). The reason for differences in palmitoyl-CoA sensitivity may be due to the differences in the antenna domain. Because these allosteric regulators do no affect bacterial GDH, it appears that this regulation evolved first and concomitantly with the antenna feature.

Like bacterial GDH, tGDH is insensitive to both GTP and leucine regulation. Even at millimolar concentrations, GTP did not inhibit tGDH (Figure 4C). This is not unexpected because, relative to mammalian GDH, there is a loss in the γ-phosphate-binding environment in Ciliate GDH (arrow 1−3 of Figure 2). In addition, tGDH is also insensitive to activation by leucine (Figure 4D). There is a slight increase in the apparent activity of tGDH at 20 mM leucine, but this is likely due to the fact that leucine is also a weak substrate for GDH. This suggests that GTP and leucine regulation are relatively newly acquired traits in animals. These results are particularly interesting in that both leucine and GTP regulation have been shown to be important in GDH-linked regulation of insulin secretion (*39*−*42*).

While is clear that tGDH is regulated by ADP and palmitoyl-CoA, it was not clear whether these regulators exhibited any interplay. As shown in Figure 4E, wild-type bGDH is strongly inhibited by palmitoyl-CoA, and this inhibition is completely abrogated by ADP at about 100 μM. However, in tGDH, ADP does not seem to be able to overcome palmitoyl-CoA inhibition to the same extent. This is somewhat consistent with the fact that tGDH is less sensitive to palmitoyl-CoA and suggests that the interplay between these modulators is not as fully developed as it is in mammalian GDH. Furthermore, this suggests that the Ciliates created this form of allosteric regulation but that it continued to be refined by animals, perhaps through further evolution of the antenna structure.

The Binding of TNP-ADP to bGDH and the R463A Mutant of hGDH. Our previous studies showed that the R463A mutation did not affect the structure of hGDH, but it did abrogate ADP activation (*8*). In our model of ADP activation, we propose that ADP does not lock the enzyme into an activated state but rather facilitates the opening of the catalytic cleft to release the product. This, we propose, is mediated by interaction between R463 on the pivot helix and the bound ADP as the catalytic cleft opens. Therefore, this mutation would not be expected to affect ADP binding but would be unable to activate without the interaction with R463. However, the fact that tGDH has a VAL at the

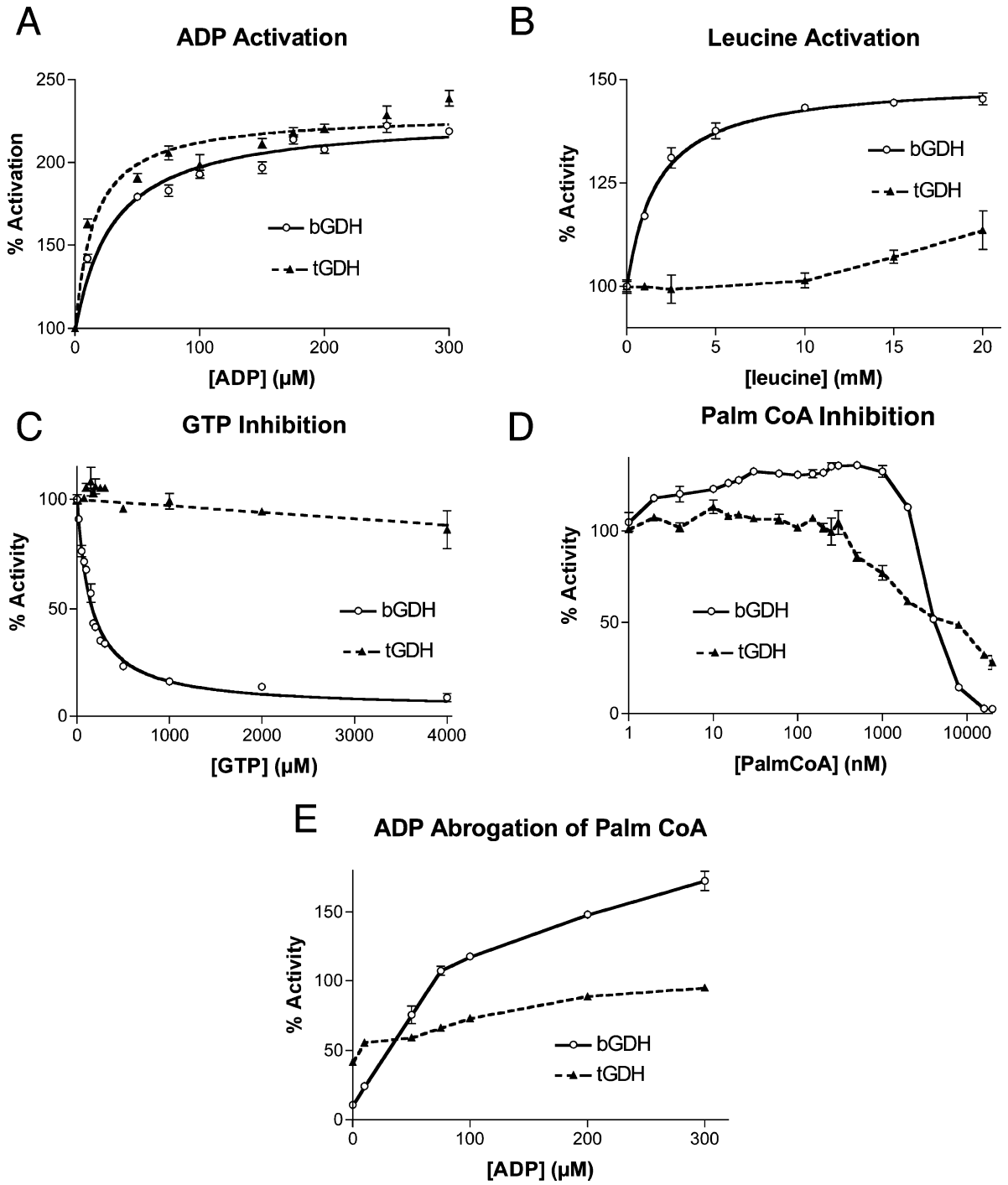

FIGURE 4: Allosteric regulation of tGDH activity in the oxidative deamination reaction. (A−D) Effects of known mammalian allosteric regulators on purified bGDH and tGDH. Note that tGDH is not sensitive to either leucine or GTP regulation, but the effects of ADP are nearly identical to mammalian GDH. In the case of palmitoyl-CoA (E), tGDH is less sensitive than mammalian GDH. It should be noted that very low concentrations of palmitoyl-CoA appear to slightly activate bGDH under these conditions. This is not observed in the reductive amination reaction (see Figure 5D). To further probe the ADP/palmitoyl-CoA regulation, the abrogation of palmitoyl-CoA regulation was examined (E). As shown here, ADP is more effective at removing palmitoyl-CoA inhibition in mammalian GDH than in tGDH. A summary of the curve-fitting analyses is shown in Table 5.

corresponding position for R463 yet is still activated by ADP calls into some question as to whether R463A might, in fact, block ADP binding. Therefore, we measured ADP binding to the R463A mutant of hGDH using the fluorescent ADP analogue, TNP-ADP. TNP-ADP has been previously shown to bind to GDH and causes similar activation as authentic ADP (*30*). As shown in Figure 5, the fluorescence of TNP-ADP is enhanced upon binding to the enzyme. It is also clear that the binding affinity of TNP-ADP to the R463A mutant is identical to that of wild-type bGDH. Interestingly, the maximum fluorescence enhancement appears to be almost twice as large in wild-type enzyme compared to that of the R463A mutant. This is not entirely surprising because the R463A mutation is expected to change the environment around the TNP moiety. Therefore, all of the data presented to date are consistent with our proposed mechanism for ADP activation. However, it is not clear how tGDH is activated by ADP when it has a VAL at the position equivalent to

Table 5: Summary of Inhibition and Activation Constants for the Various Forms of GDH[a]

enzyme	ligand	K_a	A_{max} (%)	K_i	I_{max} (%)
bGDH	ADP	31(6) μM	128(5)		
	GTP			150(10) μM	96(2)
	leucine	1.7(0.2) mM	50(1.2)		
tGDH	ADP	15(3) μM	130(4)		
	GTP			NC	NC
	leucine	NC	NC		
hGDH	ADP	18(1.0) μM	129(2)		
	GTP			0.1(0.01) μM	97(2)
	leucine	2.4(0.7) mM	73(9)		
hybrid	ADP	47(20) μM	164(28)		
	GTP			0.87(0.29) μM	95(5)
	leucine	0.43(0.14) mM	28(2)		
antenna-less	ADP	NC	NC		
	GTP			NC	NC
	leucine	0.52(0.20) mM	39(4)		

[a] These values are derived from nonlinear regression analysis of the data shown in Figures 4, 6, and 7. For leucine and ADP activation, the following equation was used: $V = (100\% + A_{max}[\text{leucine or ADP}])/(K_a + [\text{leucine or ADP}])$, where V, A_{max}, and K_a represent the steady-state velocity, maximum activation, and apparent allosteric ligand disassociation constant, respectively. For GTP inhibition, the following equation was used for fitting: $V = (100\% - I_{max}[\text{GTP}])/(K_i + [\text{GTP}])$, where I_{max} and K_i represent the maximum inhibition and apparent GTP disassociation constant, respectively. NC denotes the lack of convergence during fitting. It should also be noted that the analyses of the palmatoyl CoA data are not shown because the biphasic curves could not be satisfactorily fitted to a two-site binding equation.

R463. It is possible that the alignment shown in Figure 2 is off in this region or that the mechanism of ADP activation in tGDH is somewhat different compared to mammalian GDH. In either case, these possible differences may lead to the relative inability of ADP to reverse the effects of palmitoyl-CoA inhibition in tGDH.

Effects of Allosteric Regulators on an Antenna-less Form of hGDH. It has been shown that bacterial GDH is unregulated (*1*) and also lacks the antenna structure (*2*, *6*). Our previous structural studies have shown that ADP and GTP regulatory sites lie on the main body of the enzyme (Figure 1) and not on the antenna (*8*, *9*). Therefore, the possible role of the antenna in allosteric regulation remained unclear. A number of HI/HA mutations lie in the antenna even though those residues are not involved in the binding of regulatory ligands (*43*). To directly ascertain the role of the antenna in allosteric regulation, the antenna was genetically removed in hGDH and replace with the corresponding short loop from cGDH. As shown in Figure 6, this has a profound effect on the regulation of hGDH. Even though the antenna does not contact either the GTP or ADP sites (*9*), the removal of the antenna eliminates the regulation by both ligands. From our previous studies, none of the HI/HA mutations were shown to affect palmitoyl-CoA inhibition (*31*), whereas here, it is apparent that the removal of the antenna eliminates this regulation. Interestingly, neither the HI/HA mutations (*31*) nor the loss of the antenna domain affects leucine activation. Together, this implies that the antenna is crucial for ADP, GTP, and palmitoyl-CoA regulation but that leucine activation occurs via a separate mechanism. It is possible that leucine activation is due to it binding to the active site and directly interfering with abortive complex formation or facilitating product release. Nevertheless, it is apparent that leucine activation is not dependent upon the antenna and that *T. thermophilia* did not apparently need to evolve such regulation.

Effects of Allosteric Regulators on a Ciliate/hGDH Hybrid. The results described above demonstrate that the antenna is crucial for allosteric regulation. However, it is not clear whether the antenna in tGDH has evolved enough to communicate all of the allosteric regulation normally found in mammalian GDH. To directly test for this, the antenna of hGDH was replaced with Ciliate (paramecium) GDH. As shown in Figure 7, the antenna is functionally similar but not identical to the normal mammalian antenna. ADP regulation of the hybrid enzyme closely mirrors that of wild-type hGDH (Figure 7A). This is consistent with the results shown in Figure 4A, showing that ADP regulation of tGDH is the same as mammalian GDH. Figure 7B shows that leucine can activate the hybrid enzyme but to a slightly lesser extent than wild-type hGDH. This is not surprising given the fact that removal of the antenna did not abrogate leucine activation but did dampen its effects. However, as shown in Figure 7C, it is apparent that the Ciliate antenna can communicate GTP inhibition even though tGDH in its entirety is not regulated by GTP. It is important to note, however, that the apparent binding efficacy is about 1 order of magnitude weaker in the hybrid compared to wild-type mammalian GDH. Similarly, the hybrid enzyme is inhibited by palmitoyl-CoA, but the efficacy is at least 1 order of magnitude weaker than the wild type. Interestingly, tGDH

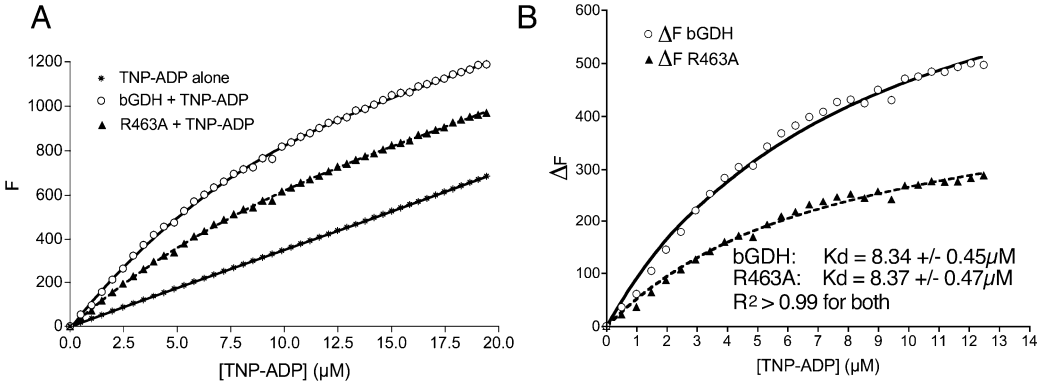

FIGURE 5: Binding of TNP-ADP to bGDH and the R463A mutant of hGDH. (A) Fluorescence of sequential additions of TNP-ADP to the buffer, bGDH, and R463A after correcting inner-filter effects. Note the fluorescence enhancement upon binding to the enzyme. (B) ΔF ($F_{TNP-ADP\cdot GDH} - F_{TNP-ADP}$) at varying concentrations of TNP-ADP. The lines represent the results of nonlinear curve fitting to the equilibrium binding equation.

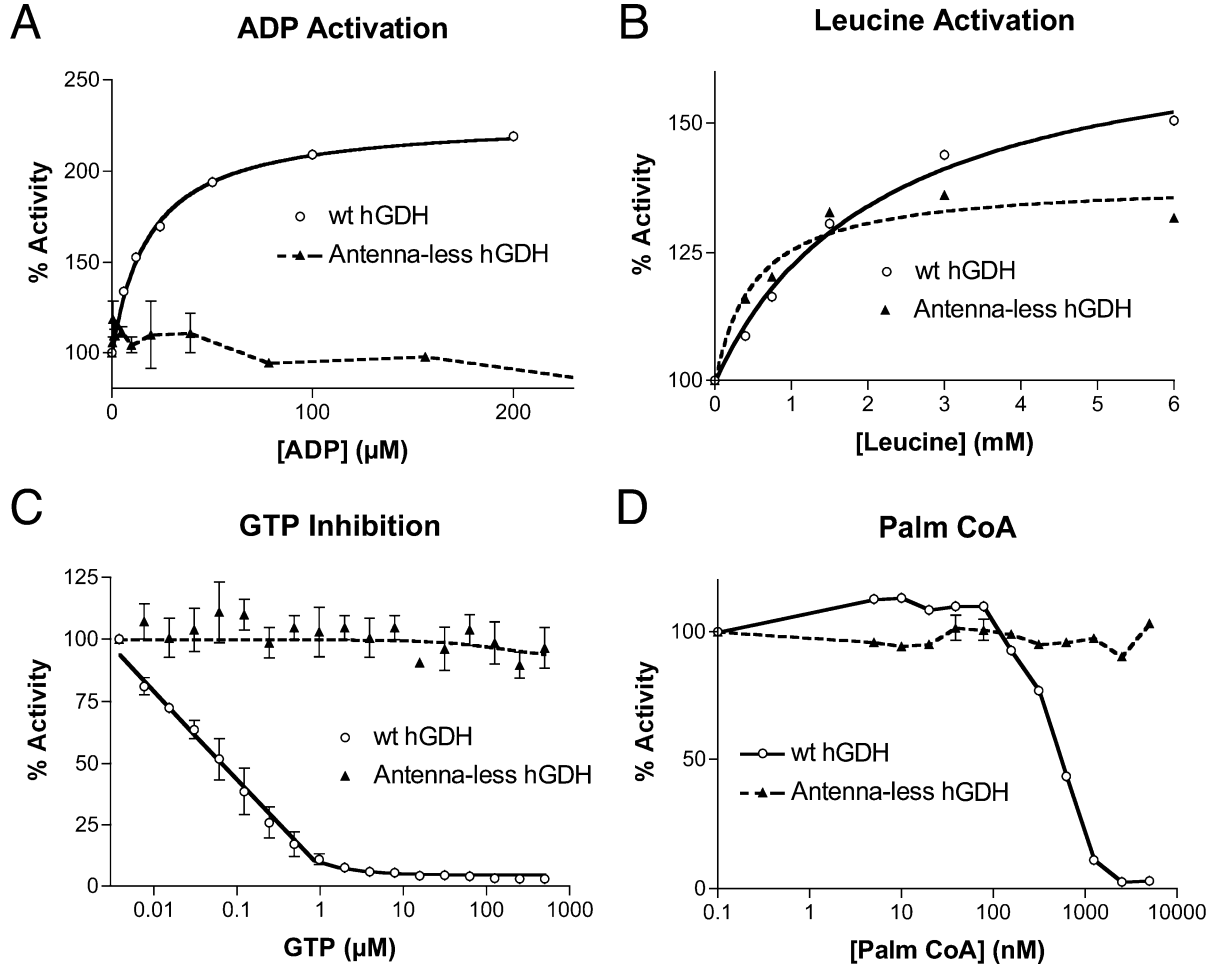

FIGURE 6: Effects of the antenna deletion mutation on mammalian GDH regulation in the reductive amination reaction. As shown here, deletion of the antenna eliminates ADP activation (A), GTP inhibition (C) and palmitoyl-CoA inhibition (D). While this form of hGDH is still activated by leucine, its effects are markedly dampened (B). A summary of the curve-fitting analyses is shown in Table 5.

was also found to have a dampened response to palmitoyl-CoA compared to mammalian GDH.

CONCLUSIONS

These results show that the antenna and allostery evolved in steps during the development of multicellular animals.

ADP Activation. ADP activation appears to have evolved concomitantly with the antenna in the Ciliates. It is clear that this is the most primitive form of allosteric activation, and the antenna-less mutant clearly demonstrates that it is dependent upon the antenna. This is despite the fact that ADP binds directly beneath the pivot helix and does not contact any portion of the antenna. Interestingly, ADP activation alone appears to have been fully evolved in the Ciliates. One possible interpretation for this activation is that, at this stage of evolution, the Ciliates found it necessary to turn on amino acid catabolism when the energy state of the mitochondria was low. However, the interplay between ADP and palmitoyl-CoA regulation may have been further refined in mammals. ADP effects on animal GDH are very complex (*10*). In the absence of other regulators such as GTP, ADP appears to mainly activate the enzyme at high substrate concentrations, where abortive complexes are expected to make product release the rate-limiting step. Therefore, the loss of ADP activation when the antenna is removed could be indirectly due to the effects on abortive complex formation. However, previous work suggests that even bacterial GDH exhibits substrate and coenzyme inhibition (*38*), and therefore, the antenna may not be relevant to abortive complex formation. Finally, as shown in Figure 4E, the main role of ADP *in vivo* may not be so much activation of the enzyme on its own but rather the abrogation of the effects of other allosteric regulators such as palmitoyl-CoA and GTP.

Palmitoyl-CoA Inhibition. Palmitoyl-CoA inhibition is the most primitive form of allosteric inhibition and appears to also be dependent upon the antenna domain. Previous studies have shown that mutations in the GTP- and ADP-binding regions do not affect palmitoyl-CoA inhibition (*31*). However, it is clearly shown here that removal of the antenna completely abrogates palmitoyl-CoA inhibition. Further, transplanting the Ciliate antenna onto hGDH attenuates the palmitoyl-CoA response of mammalian GDH, making it more similar to tGDH. While we do not yet know the location of the palmitoyl-CoA-binding site, it is tempting to speculate that palmitoyl-CoA might be binding to the antenna domain and inhibited by affecting the conformational changes associated with the opening and closing of the catalytic cleft (*7*).

Leucine Activation. Leucine activation appears to be a more recent evolutionary development. It is clear that tGDH is not activated by leucine and that deletion of the antenna in hGDH does not affect leucine activation. This demon-

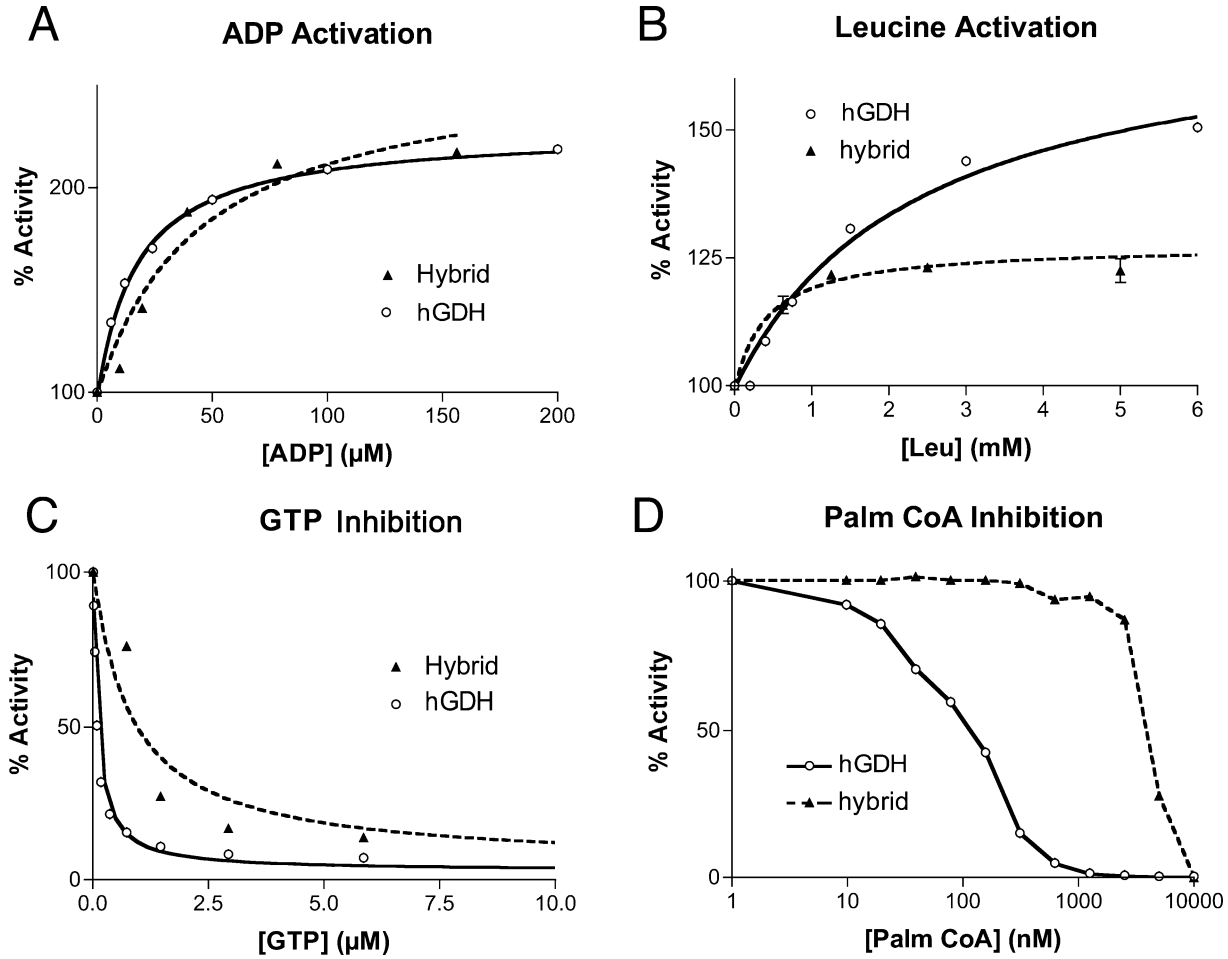

FIGURE 7: Effects of replacing the antenna in hGDH with that from pGDH. This hybrid enzyme appears to have the full complement of mammalian allosteric regulation. While the effects of ADP on the hybrid enzyme are identical to those of wild-type hGDH (A), this mutation appears to affect the extent of leucine activation (B) and the apparent binding constants for both GTP and palmitoyl-CoA (C and D). A summary of the curve-fitting analyses is shown in Table 5.

strates that leucine does not bind to or depend on the antenna domain for activity. Therefore, it appears that leucine regulation was not a driving force for the evolution of the antenna and appears to have been "layered on" after its formation. It is important to note that leucine has been shown to stimulate insulin secretion presumably via GDH activation (*41*), and therefore, a different set of evolutionary pressures appear to have been at work creating leucine activation.

GTP Inhibition. It is also clear from these results that the antenna was not evolved to facilitate GTP inhibition because tGDH is completely insensitive to GTP. However, as the antenna deletion and a number of the HI/HA mutations have shown (*31*, *40*, *43*), the antenna is clearly essential to communicate this inhibition. The hybrid studies also show that the Ciliate antenna is fully capable of facilitating this inhibition but that the Ciliates apparently did not find the need to develop the appropriate GTP-binding site at the base of the antenna domain. Therefore, it is clear that the Ciliates developed the architecture necessary for GTP inhibition prior to its evolutionary need in animals. One possible reason for the evolution of GTP inhibition comes from our previous studies on the HI/HA syndrome that demonstrate how crucial the inhibition of GDH by GTP is in the maintenance of insulin homeostasis in mammals (*32*).

SUMMARY

Together, these results suggest a process of GDH evolution. Evolving away from plants, fungi, bacteria, and other protists, the Ciliates created this ~50-residue antenna domain. The antenna is not involved in the ADP-binding site (*8*), but the inner hydrophobic regions of this domain may contain the palmitoyl-CoA-binding site. Nevertheless, the antenna itself is crucial for the creation of both palmitoyl-CoA and ADP regulation. Our previous structural studies have shown that the antennae from subunits within the trimer intertwine and undergo conformational changes as the active-site clefts open and close during the catalytic cycle (*6*−*9*). While the exact mechanism for how the antenna plays such a crucial role in allostery is not clear, the effects of the antenna deletion mutation make it apparent that the subunit communication that occurs during allosteric regulation must be occurring within the trimer rather than across the trimer−trimer interface.

The results shown here demonstrate that the Ciliates created an antenna that is fully capable of communication and that all of the allosteric regulation subsequently evolved in mammals but did not find the need for such regulation. The hybrid studies show that the Ciliates could have used their antennae for GTP regulation, but from the sequence

alignments, it is apparent that they had not yet evolved the GTP-binding site on the top of the NAD-binding domain to accommodate it. However, the hybrid is less sensitive to GTP inhibition than wild-type hGDH, suggesting that the antenna itself was further refined in mammals. This is consistent with the differences between animals and Ciliates in the sequence and length of the antenna.

Exaptation is a term coined to describe the adoption of a characteristic used in an ancestral form into a new, different use in a descendant form (*44*). For example, ancestors to birds were flightless, reptile-like creatures with very light "honeycomb" bones. Through exaptation, the bones of these "flightless birds" became the lightweight skeletal specializations that were later used to accommodate flight in "true birds." GTP inhibition, therefore, appears to be an example of exaptation at the molecular level because the antenna was not originally evolved in the Ciliates for the purpose of GTP regulation. However, mammals used this existing structure to add an additional layer of regulation, GTP inhibition. GTP inhibition is clearly important as is made evident by the fact that the loss of this regulation is the root cause of the HI/HA syndrome (*45*).

While these results suggest a process for the evolution of allosteric regulation of GDH, it does not explain why this evolution was first initiated in the Ciliates. The development of palmitoyl-CoA regulation may be an important clue as to this evolutionary pressure. The results presented here demonstrate that the first inhibitor for GDH was palmitoyl-CoA and that this regulation is entirely dependent upon the antenna. The reason for the appearance of this regulation may be due to the changes in organelle function as the Ciliates and animals evolved away from the other kingdoms. In plants (*46*, *47*) and fungi (*48*), fatty acid oxidation occurs entirely in the peroxisomes. In contrast, animals perform β-oxidation of medium and long chain fatty acids mainly in the mitochondria, while the very long chain fatty acids are catabolized in the peroxisomes (*49*, *50*). The Ciliates are somewhere between these two groups with β-oxidation occurring in both the peroxisomes and the mitochondria (*51*, *52*). Indeed, it was suggested in this earlier work that *T. thermophilia* might have developed new metabolic regulations in the mitochondria that allowed for the evolutionary loss of glyoxylate cycle enzymes from the peroxisomes (*51*). Interestingly, Kinetoplastida (e.g., Trypanosome) GDH does not have an antenna and is very homologous to bacterial GDH [70% identical to *E. coli* (*53*)]. While these organisms are also members of the Protista kingdom, their metabolic compartmentalization is more like plants with their specialized peroxisomes called glycosomes (*54*, *55*). Therefore, we propose that the antenna evolved to link fatty acid and amino acid catabolism in the mitochondria. The evolutionary pressure for this linkage came from the fact that, as animals began to evolve, fatty oxidation began to move from the peroxisomes to the mitochondria. Combined with ADP activation, the organism could now activate amino acid oxidation only when the energy state of the mitochondria was low and alternative energy sources such as fatty acids had been depleted.

We propose that the next evolutionary step from the Ciliate to the highly complex mammalian form of GDH is an example of exaptation where the antenna, derived from the evolutionary pressures caused by changes in organelle function, is further developed to link GDH activity with insulin homeostasis. As animals evolved, the mitochondria became the major location for oxidation. In particular, the majority of fatty acid oxidation moved to the mitochondria and became entirely controlled by the carnitine palmitoyl transferase system that is in turn regulated by glucose and insulin levels (*56*). Similarly, as GDH evolved, GTP inhibition and leucine activation were added to the list of regulators. In the case of GTP, the results presented here clearly demonstrate that this inhibition is entirely dependent upon the recently evolved antenna. From studies on the HI/HA syndrome, it is clear that the loss of GTP inhibition of GDH causes a profound increase in insulin secretion. In both normal and HI/HA pancreatic tissue, leucine stimulates insulin secretion through the activation of GDH (*41*). Furthermore, it has been suggested that glutamine/glutamate acts as a secondary messenger in glucose-stimulated insulin exocytosis and GDH plays a crucial role in regulating its intracellular concentrations (*41*, *57*, *58*). It appears, therefore, that the creation of GTP and leucine regulation was not accidental but was necessary for insulin homeostasis. Therefore, we propose that the antenna and associated regulation evolved in response to changes in organelle function and was then used for regulation of insulin homeostasis in an example of exaptation at the molecular level. Studies are underway to test some of these ideas by better understanding why the Ciliates did not need the GTP and leucine regulation and what would be the consequence of losing ADP and palmitoyl-CoA regulation.

ACKNOWLEDGMENT

The authors especially thank Dr. James Forney, Purdue University, for assisting us in establishing the *T. thermophilia* cell lines and protocols in our laboratory. Figure 1 was created using MolViewX [http://www.danforthcenter.org/smith/molview.htm (*59*)].

REFERENCES

1. Hudson, R. C., and Daniel, R. M. (1993) L-Glutamate dehydrogenases: Distribution, properties, and mechanism, *Comp. Biochem. Physiol., Part B: Biochem. Mol. Biol. 106*, 767−792.
2. Baker, P. J., Britton, K. L., Engel, P. C., Farrantz, G. W., Lilley, K. S., Rice, D. W., and Stillman, T. J. (1992) Subunit assembly and active site location in the structure of glutamate dehydrogenase, *Proteins: Struct., Funct., and Genet. 12*, 75−86.
3. Knapp, S., de Vos, W. M., Rice, D., and Ladenstein, R. (1997) Crystal structure of glutamate dehydrogenase from the hyperthermophilic eubacterium *Thermotoga maritima* at 3.0 Å resolution, *J. Mol. Biol. 267*, 916−932.
4. Rice, D. W., Baker, P. J., Farrants, G. W., and Hornby, D. P. (1987) The crystal structure of glutamate dehydrogenase from *Clostridium symbiosum* at 0.6 nm resolution, *Biochem. J. 242*, 789−795.
5. Yip, K. S. P., Stillman, T. J., Britton, K. L., Artymiuk, P. J., Baker, P. J., Sedelnikova, S. E., Engel, P. C., Pasquo, A., Chiaraluce, R., Consalvi, V., Scandurra, R., and Rice, D. W. (1995) The structure of *Pyrococcus furiosus* glutamate dehydrogenase reveals a key role for ion-pair networks in maintaining enzyme stability at extreme temperatures, *Structure 3*, 1147−1158.
6. Peterson, P. E., and Smith, T. J. (1999) The structure of bovine glutamate dehydrogenase provides insights into the mechanism of allostery, *Structure 7*, 769−782.
7. Smith, T. J., Schmidt, T., Fang, J., Wu, J., Siuzdak, G., and Stanley, C. A. (2002) The structure of apo human glutamate dehydrogenase details subunit communication and allostery, *J. Mol. Biol. 318*, 765−777.

8. Banerjee, S., Schmidt, T., Fang, J., Stanley, C. A., and Smith, T. J. (2003) Structural studies on ADP activation of mammalian glutamate dehydrogenase and the evolution of regulation, *Biochemistry 42*, 3446−3456.
9. Smith, T. J., Peterson, P. E., Schmidt, T., Fang, J., and Stanley, C. (2001) Structures of bovine glutamate dehydrogenase complexes elucidate the mechanism of purine regulation, *J. Mol. Biol. 307*, 707−720.
10. Bailey, J. S., Bell, E. T., and Bell, J. E. (1982) Regulation of bovine glutamate dehydrogenase, *J. Biol. Chem. 257*, 5579−5583.
11. Frieden, C. (1965) Glutamate dehydrogenase VI. Survey of purine nucleotides and other effects on the enzyme from various sources, *J. Biol. Chem. 240*, 2028−2037.
12. George, S. A., and Bell, J. E. (1980) Effects of adenosine 5′-diphosphate on bovine glutamate dehydrogenase: Diethyl pyrocarbonate modification, *Biochemistry 19*, 6057−6061.
13. Iwatsubo, M., and Pantaloni, D. (1967) Regulation De L′ Activite′ De La glutamate dehydrogenase par les effecteurs GTP et ADP: ETUDE par "stopped flow", *Bull. Soc. Chem. Biol. 49*, 1563−1572.
14. Koberstein, R., and Sund, H. (1973) The influence of ADP, GTP, and L-glutamate on the binding of the reduced coenzyme to beef-liver glutamate dehydrogenase, *Eur. J. Biochem. 36*, 545−552.
15. Dieter, H., Koberstein, R., and Sund, H. (1981) Studies of glutamate dehydrogenase. The interaction of ADP, GTP, and NADPH in complexes with glutamate dehydrogenase, *Eur. J. Biochem. 115*, 217−226.
16. Frieden, C. (1959) Glutamic dehydrogenase I. The effect of coenzyme on the sedimentation velocity and kinetic mechanism, *J. Biol. Chem. 234*, 809−814.
17. Frieden, C. (1959) Glutamic dehydrogenase II The effect of various nucleotides on the association-disassociation and kinetic properties, *J. Biol. Chem. 234*, 815−819.
18. Limuti, C. M. (1983) in *Department of Biochemistry*, University of Rochester, Rochester, New York.
19. Bayley, P. M., and O'Neill, T. J. (1980) The binding of oxidised coenzyme to bovine-liver glutamate dehydrogenase studied by circular-difference spectroscopy, *Eur. J. Biochem. 112*, 521−531.
20. Batra, S. P., and Colman, R. F. (1984) Affinity labeling of the reduced diphosphopyridine nucleotide inhibitory site of glutamate dehydrogenase by 6-[(4-bromo-2,3-dioxobutyl)thio]-6-deaminoadenosine 5′-diphosphate, *Biochemistry 23*, 4940−4946.
21. Batra, S. P., and Colman, R. F. (1986) Isolation and identification of cysteinyl peptide labeled by 6-[(4-bromo-2,3-dioxobutyl)thio]-6-deaminoadenosine 5′-diphosphate in the reduced diphosphopyridine nucleotide inhibitory site of glutamate dehydrogenase, *Biochemistry 25*, 3508−3515.
22. Yielding, K. L., and Tomkins, G. M. (1961) An effect of L-leucine and other essential amino acids on the structure and activity of glutamate dehydrogenase, *Proc. Natl. Acad. Sci. U.S.A. 47*, 983.
23. Prough, R. A., Culver, J. M., and Fisher, H. F. (1973) The mechanism of activation of glutamate dehydrogenase-catalyzed reactions by two different, cooperatively bound activators, *J. Biol. Chem. 248*, 8528−8533.
24. Fahien, L. A., and Kmiotek, E. (1981) Regulation of glutamate dehydrogenase by palmitoyl-coenzyme A, *Arch. Biochem. Biophys. 212*, 247−253.
25. Tomkins, G. M., and Yielding, K. L., and Curran, J. F. (1962) The influence of diethylstilbestrol and adenosine diphosphate on pyridine nucleotide coenzyme binding by glutamic dehydrogenase, *J. Biol. Chem. 237*, 1704−1708.
26. Weinzimer, S. A., Stanley, C. A., Berry, G. T., Yudkoff, M., Tuchman, M., and Thornton, P. S. (1997) A syndrome of congenital hyperinsulinism and hyperammonemia, *J. Pediatr. 130*, 661−664.
27. Stanley, C. A., Lieu, Y. K., Hsu, B. Y. L., Burlina, A. B., Greenberg, C. R., Hopwood, N. J., Perlman, K., Rich, B. H., Zammarchi, E., and Poncz, M. (1998) Hyperinsulinism and hyperammonemia in infants with regulatory mutations of the glutamate dehydrogenase gene, *N. Engl. J. Med. 338*, 1352−1357.
28. Gao, Z., Li, G., Najafi, H., Wolf, B. A., and Matschinsky, F. M. (1999) Glucose regulation of glutaminolysis and its role in insulin secretion, *Diabetes 48*, 1535−1547.
29. Matschinsky, F. M. (1996) Banting lecture 1995. A lesson in metabolic regulation inspired by the glucokinase glucose sensor paradigm, *Diabetes 45*, 223−241.
30. Jacobson, M. A., and Colman, R. F. (1983) Resonance energy transfer between the adenosine 5′-diphosphate site of glutamate dehydrogenase and a guanosine 5′-triphosphate site containing a tyrosine labeled with 5′-(*p*-fluorosulfonyl benzoyl)-1,*N*6-ethenoadenosine, *Biochemistry 22*, 4247−4257.
31. Fang, J., Macmullen, C., Smith, T. J., and Stanley, C. A. (2001) Expression, purification, and characterization of human glutamate dehydrogenase (GDH) regulatory mutations associated with a dominantly expressed congenital hyperinsulinism/hyperammonemia syndrome, *Biochem. J. 363*, 81−87.
32. Stanley, C. A. (2000) in *Genetic Insights in Paediatric Endocrinology and Metabolism* (O'Rahilly, S., and Dunger, D. B., Eds.) pp 23−30, BioScientifica, Ltd., Bristol, U.K.
33. Goldin, B. R., and Frieden, C. (1971) Effect of trinitrophenylation of specific lysyl residues on the catalytic, regulatory, and molecular properties of bovine liver glutamate dehydrogenase, *Biochemistry 10*, 3527−3534.
34. Dalziel, K., and Engel, P. C. (1968) Antagonistic homotropic interactions as a possible explanation of coenzyme activation of glutamate dehydrogenase, *FEBS Lett. 1*, 349−352.
35. Engel, P., and Dalziel, K. (1969) Kinetic studies of glutamate dehydrogenase with glutamate and norvaline as substrates, *Biochem. J. 115*, 621−631.
36. Bell, J. E., and Dalziel, K. (1973) A conformational transition of the oligomer of glutamate dehydrogenase induced by half-saturation with NAD^+ or $NADP^+$, *Biochim. Biophys. Acta 309*, 237−242.
37. Bell, E. T., LiMuti, C., Renz, C. L., and Bell, J. E. (1985) Negative cooperativity in glutamate dehydrogenase. Involvement of the 2-position in the induction of conformational changes, *Biochem. J. 225*, 209−217.
38. Syed, S. E.-H., Engel, P. C., and Parker, D. M. (1991) Functional studies of a glutamate dehydrogenase with known three-dimensional structure: Steady-state kinetics of the forward and reverse reactions catalysed by the NAD^+-dependent glutamate dehydrogenase of *Clostridium symbiosum*, *Biochim. Biophys. Acta 1115*, 123−130.
39. Hsu, B. Y. L., Kharlip, J., Fang, J., Poncz, M., Glaser, B., and Stanley, C. A. (1998) "Leucine sensitive hypoglycemia" caused by dominantly inherited mutations of glutamate dehydrogenase, *Pediatr. Res. 43*, 78A (SPR meeting abstract).
40. Stanley, C. A., Fang, J., Kutyna, K., Hsu, B. Y., Ming, J. E., Glaser, B., and Poncz, M. (2000) Molecular basis and characterization of the hyperinsulinism/hyperammonemia syndrome: Predominance of mutations in exons 11 and 12 of the glutamate dehydrogenase gene. HI/HA contributing investigators, *Diabetes 49*, 667−673.
41. Li, C., Najafi, H., Daikhin, Y., Nissim, I., Collins, H. W., Yudkoff, M., Matschinsky, F. M., and Stanley, C. A. (2002) Regulation of leucine stimulated insulin secretion and glutamine metabolism in isolated rat islets, *J. Biol. Chem. 278*, 2853−2858.
42. Kelly, A., Ng, D., Ferry, R. J., Grimberg, A., Koo-Mccoy, S., Thornton, P. S., and Stanley, C. A. (2001) Acute insulin responses to leucine in children with the hyperinsulinism/hyperammonemia syndrome, *J. Clin. Endocrinol. Metab. 86*, 3724−3728.
43. Stanley, C. A., Fang, J., Kutyna, K., Hsu, B. Y. L., Ming, J. E., Glaser, B., and Poncz, M. (2000) Molecular basis and characterization of the hyperinsulinism/hyperammonemia syndrome of the glutamate dehydrogenase gene, *Diabetes 49*, 667−673.
44. Gould, S. J., and Vrba, E. S. (1982) Exaptation−A missing term in the science of form, *Paleobiology 8*, 4−15.
45. MacMullen, C., Fang, J., Hsu, B. Y. L., Kelly, A., deLonlay-Debeney, P., Saudubray, J. M., Ganguly, A., Smith, T. J., and Stanley, C. A. (2001) The hyperinsulinism/hyperammonemia contributing investigators. Hyperinsulinism/hyperammonemia syndrome in children with regulatory mutations in the inhibitory guanosine triphosphate-binding domain of glutamate dehydrogenase, *J. Clin. Endocrinol. Metab. 86*, 1782−1787.
46. Gerhardt, B. (1992) Fatty acid degradation in plants, *Prog. Lipid Res. 31*, 417−446.
47. Kindl, H. (1993) Fatty acid degradation in plant peroxisomes: Function and biosynthesis of enzymes involved, *Biochimie 75*, 225−230.
48. Erdmann, R., Veenhuis, M., and Kunau, W. H. (1997) Peroxisomes: Organelles at the crossroads, *Trends Cell Biol. 7*, 400−407.
49. Reddy, J. K., and Mannaerts, G. P. (1994) Peroxisomal lipid metabolism, *Annu. Rev. Nutr. 14*, 343−370.
50. Hashimoto, T. (1999) Peroxisomal β-oxidation enzymes, *Neurochem. Res. 24*, 551−563.
51. Muller, M., Hogg, J. F., and De Duve, C. (1968) Distribution of tricarboxylic acid cycle enzymes and glyoxylate cycle enzymes

between mitochondria and peroxisomes in *Tetrahymena pyriformis*, *J. Biol. Chem. 243*, 5385−5395.
52. Blum, J. J. (1973) Localization of some enzymes of β-oxidation of fatty acids in the peroxisomes of *Tetrahymena*, *J. Protozool. 20*, 688−692.
53. Barderi, P., Campetella, O., Frasch, A. C. C., Santome, J. A., Hellman, U., Pettersson, U., and Cazzulo, J. J. (1998) The $NADP^+$-linked glutamate dehydrogenase from *Trypanosoma cruzi*: Sequence, genomic organization, and expression, *Biochem. J. 330*, 951−958.
54. Michels, P. A. M., Hannaert, V., and Bringaud, F. (2000) Metabolic aspects of glycosomes in *Trypanosomatidae*—New data and views, *Parasitol. Today 16*, 482−489.
55. Hannaert, V., Saavedra, E., Duffieux, F., Szikora, J.-P., Rigden, D. J., Michels, P. A. M., and Opperdoes, F. R. (2003) Plant-like traits associated with metabolism of *Trypanosoma* parasites, *Proc. Natl. Acad. Sci. U.S.A. 100*, 3205−3213.
56. Rasmussen, B. B., and Wolfe, R. R. (1999) Regulation of fatty acid oxidation in skeletal muscle, *Annu. Rev. Nutr. 19*, 463−484.
57. Maechler, P., and Wollheim, C. B. (1999) Mitochondrial glutamate acts as a messenger in glucose-induced insulin exocytosis, *Nature 402*, 685−689.
58. Li, C., Buettger, C., Kwagh, J., Matter, A., Daihkin, Y., Nissiam, I., Collins, H. W., Yudkoff, M., Stanley, C. A., and Matschinsky, F. M. (2004) A signaling role of glutamine in insulin secretion, *J. Biol. Chem. 279*, 13393−13401.
59. Smith, T. J. (2004) MolViewX: A molecular visualization program for the Macintosh OS X system, *J. Appl. Crystallogr. 37*, 654−657.

BI048817I